32nd URSI GASS, Montreal, 19-26 August 2017

Effective solar indices for ionospheric modeling: a proposal for a real time IRI

A. Pignalberi[(1)], M. Pezzopane[(2)], R. Rizzi[(1)], and I. Galkin [(3)]
(1) Dipartimento di Fisica e Astronomia, Università di Bologna "Alma Mater Studiorum", Bologna, Italy.
(2) Istituto Nazionale di Geofisica e Vulcanologia, Rome, Italy.
(3) Center for Atmospheric Research, University of Massachusetts, Lowell, Massachusetts, USA

Abstract

A method to real-time update the IRI model through data assimilated by a European ionosonde network is proposed, described and statistically evaluated under a severe geomagnetic event (the St.Patrick storm occurred on March 17 2015), comparing the corresponding output with the ones by IRI and IRTAM models. This method, called IRI UP (International Reference Ionosphere UPdate), relies on the foF2 and M(3000)F2 ionospheric characteristics routinely recorded by a network of 12 European ionosonde stations. The real-time assimilated data are used to calculate updated IRI's indices IG_{12} and R_{12} (identified as IG_{12eff} and R_{12eff}) for every station's point, that are used to calculate maps of these indices through the universal Kriging method. Five variogram models are used and statistically tested to verify which of these perform better for each effective index. Maps of these updated indices are used as input for the IRI model, which gives as output updated values of foF2 and hmF2. In order to evaluate the ability of the proposed method to catch fast-time and small-scale changes that are usual under disturbed conditions, statistical quantities are calculated for two test stations (not considered in the assimilation process), Fairford and San Vito, for the IRI model with the STORM option set to on, and for IRI UP and for IRTAM methods. The method here proposed turns out to be very effective, with significant improvements regarding foF2 characteristic and slight improvements for hmF2. Important improvements have been verified also for quiet and moderate disturbed conditions.

1. Introduction

It is a matter of fact that the critical frequencies of the ionospheric layers depend in a systematic way on measurable quantities related to solar radiation and to the neutral atmosphere composition and structure; at the same time, however, the structure and dynamics of the ionosphere are profoundly dependent on measurable quantities related to geomagnetic activity.

Ionospheric empirical climatological models, like IRI (International Reference Ionosphere, [1]), are not able to predict all the ionospheric variability, specifically under disturbed magnetic conditions. IRI includes a STORM (Storm-Time Ionospheric Correction Model) option [2] which simulates the ionospheric plasma behavior under magnetically disturbed periods, operating on foF2 and hmF2 modelled ionospheric characteristics and on the topside part of the vertical electron density profile. Despite all the efforts made to improve the behavior of the IRI model under magnetically disturbed conditions, the response of the ionosphere under severe geomagnetic storms is still a challenge, as it was recently demonstrated in [3] by doing a comparison between electron density values in the topside part of the ionosphere as measured by Swarm satellites and calculated by IRI.

The aforementioned considerations lead to the conclusion that we need an ionospheric weather model able to properly represent the ionospheric plasma variability caused by solar activity, geomagnetic activity and neutral atmosphere changes. This need has been recently recognized by the IRI community, pushing towards a Real-Time IRI use as explained in [1].

In this work we focus on models using effective solar indices, calculated thanks to the information provided by assimilated ionospheric measured parameters, to update a climatological background. Among the many data assimilation and spatial interpolation methods proposed for this purpose we focus on universal Kriging method, a version of which has been implemented.

2. Data and Methods

2.1. Ionospheric activity indexes calculation

IRI modeling of F2 layer characteristics, foF2 and M(3000)F2, relies on CCIR [4] long-term global maps. In this mapping procedures IRI uses diurnal/spherical harmonic expansions to represent the diurnal cycle of foF2 and M(3000)F2. Diurnal and spatial coefficients are calculated for two selected levels of solar activity ($IG_{12} = 0$ and $IG_{12} = 100$ for foF2, $R_{12} = 0$ and $R_{12} = 100$ for M(3000)F2). IRI model assumes that these coefficients are linearly correlated with solar activity proxies (positively between IG_{12} and foF2, negatively between R_{12} and M(3000)F2), until a threshold value set to 150 (for both indexes) beyond which foF2 and M(3000)F2 are kept constants. The F2 peak height, hmF2, in IRI is obtained by its close correlation with the propagation parameter M(3000)F2 [5]. hmF2 is dependent on R_{12}both explicitly and implicitly through M(3000)F2 and foE characteristics. Moreover, the presence of the foF2 characteristic in its formulation makes hmF2 implicitly dependent also on IG_{12}.

IRI gives the opportunity to input a user defined value for both R_{12} and IG_{12} indices to make a simulation. This means that IRI can model improved foF2 and M(3000)F2 values using updated values of IG_{12} and R_{12}.

In the method we propose the values of *fo*F2 and M(3000)F2 at one location are determined from the IRI model by using values of IG_{12eff} and R_{12eff}, instead of $IG_{12}$and R_{12}. IG_{12eff} and R_{12eff} indices are calculated through the comparison of IRI foF2 and M(3000)F2 estimates with actual measurements made by the ionosonde network. IG_{12eff} (R_{12eff}) is chosen to give the minimum square error between IRI outputs and actual measurements obtained from a grid of ionosondes, referred as assimilated stations. In this way, the two calibration parameters IG_{12eff} and R_{12eff} become both of them ionospheric activity indices. Hence, IG_{12eff} and R_{12eff} should be able to capture severe ionospheric disturbances, in spite of the causes that have generated them (solar activity, geomagnetic activity, neutral atmosphere changes, or other phenomena).

Because IG_{12eff} (R_{12eff}) values are calculated for every assimilated station, we need to interpolate these values through the chosen grid. The universal Kriging method is then used to obtain a map of IG_{12eff} and R_{12eff} on the chosen grid.

2.2. Universal Kriging interpolation method

Kriging is an advanced geostatistical procedure that, used as an interpolator, generates an estimated surface from a scattered set of punctual geophysical measurements [6]. The *experimental variogram* (or semivariogram) is the core of the Kriging method, because it allows to investigate the spatial correlation between measurements. The experimental variogram contains information about the *scale of fluctuations* of the variable and can provide clues on whether the scale of the variability is large or small. A mathematical expression, called *variogram model*, is then fitted to the points in the experimental variogram. Five different variogram models were considered: *gaussian*, *spherical* and *exponential* (that are stationary), *power* and *linear* (that are non-stationary).

The geostatistics method known as *universal kriging* (or *kriging with a drift*) is based on the *linear model* (that has not to be confused with the linear variogram model) [7]. This model is based on the reasonable assumption that the measured geophysical field displays a large-scale component of spatial variability, that can be represented with reasonable reliability as a *deterministic* function, and a small-scale spatial variability, the *stochastic* part, involving spatial correlations inferable from the variogram. In our model the deterministic part is a *2D regional linear mean* in the longitude and latitude variables.

2.3. Data selection and assimilation

The considered time period is between 9 March 2015 at 0 UT (Universal Time) and 25 March 2015 at 23 UT, a time period including the so called St. Patrick geomagnetic storm. The St. Patrick storm was the most intense geomagnetic storm observed during solar cycle 24, classified as severe and for which the *K*p index reached the maximum value of 8. In the bottom panel of Fig. 2 are shown the Dst (red line) and AE (cyan line) indices.

Hourly values of foF2, M(3000)F2, and hmF2 are used. These data were downloaded from the DIDBASE (Digital Ionogram DataBASE) through the SAO Explorer software. Fourteen ionospheric stations in the European sector, from 15°E to 45°W in longitude and from 30°N to 60°N in latitude, are selected (see Fig.1). Twelve stations were used for the assimilation process, while two (Fairford and San Vito stations) were used as test stations to verify the method performance.

3. Results and Discussion

3.1. Variogram model's statistic

For every hour of the studied time period the available values of foF2 and M(3000)F2 are used to calculate punctual IG_{12eff} and R_{12eff} values. Then, universal Kriging method is used to interpolate these values on the chosen grid using each of the five variogram models, in order to evaluate which of these gives the best results when foF2 and M(3000)F2 values recorded at the test stations are compared with those given as output by the method. For every hour we have obtained an IG_{12eff} and R_{12eff} map, like those shown in Fig.1, in which the black circles indicate the assimilated stations available for that moment, , while the red circles indicate stations for which values to be assimilated were unavailable for that moment. The two white stars in both panels of Fig. 1 indicate the geographical position of the two test stations, Fairford in the upper left corner and San Vito in the middle lower part. With the IG_{12eff} and R_{12eff} values for Fairford and San Vito geographical position, the IRI model has been run, obtaining updated values of foF2 and M(3000)F2. These updated values have been compared with those measured by the ionosondes, by means of several statistical quantities. This statistical analysis (not shown here) suggested to choose the spherical model for foF2 and the linear model for M(3000)F2 as the best methods. Thus, using the spherical method to obtain IG_{12eff} maps (by which updated foF2 values are calculated) and the linear method to obtain R_{12eff} maps (by which updated M(3000)F2 values are calculated), updated hmF2 values are also obtained.

3.2. IG_{12eff} and R_{12eff} indices

In Fig.2 the time series of IG_{12eff} (in green), IG_{12} (in blue), R_{12eff} (in green), and R_{12} (in blue), for Fairford and San Vito, are shown. The time series of the geomagnetic indices Dst (in red) and AE (in cyan), to graphically show the effects of the St.Patrick geomagnetic storm, are also reported. From Fig. 2 it clearly emerges that effective indices can catch small-temporal variations compared to the climatological counterparts, both for quiet and disturbed periods. However, the power to use an effective index occurs mainly under storm, in the main phase but also in the recovery phase, as it is evident from the IG_{12eff} and R_{12eff} time series in Fig.2.

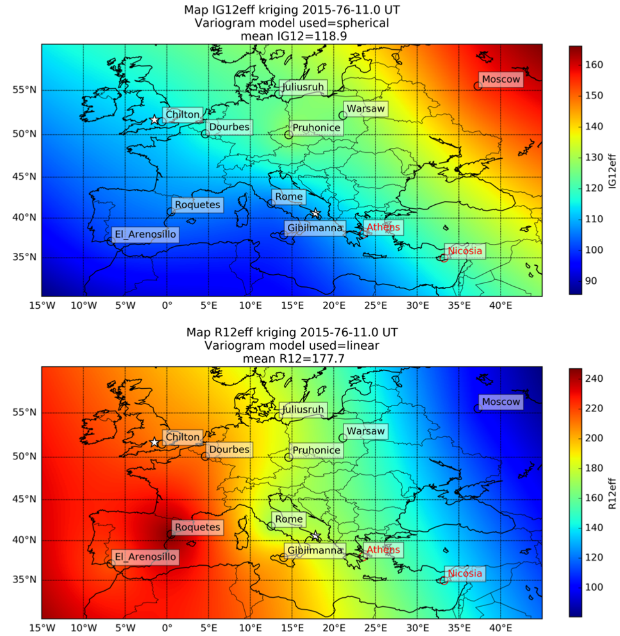

Fig 1: IG_{12eff} (top panel) and R_{12eff} (bottom panel) maps for 17 March 2015 (calendar day 76) at 11 UT.

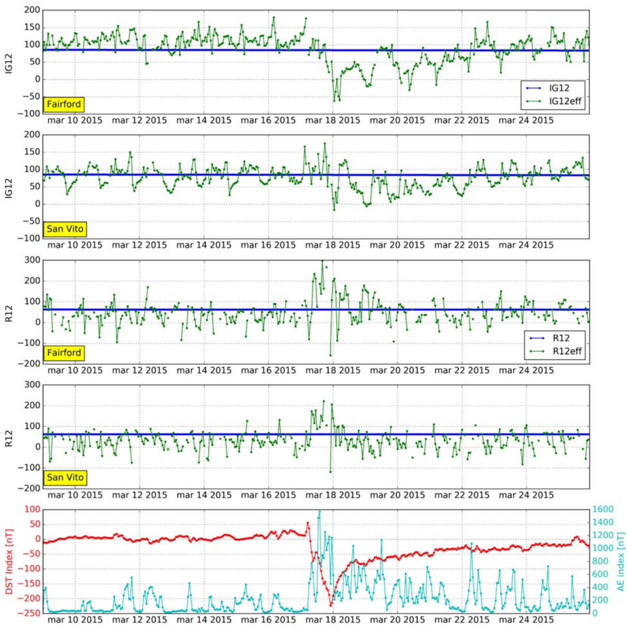

Fig 2: Time series, for the studied period, of IG_{12}, IG_{12eff}, R_{12} and R_{12eff} for Fairford and San Vito, and, in the fifth panel from the top, of the Dst (red line) and AE (cyan line) indices.

3.3. Comparison with IRI and IRTAM models

The output obtained by our method have been compared with the ones by the IRI-RTAM model (also note as IRTAM, IRI Real Time Assimilative Model, http://giro.uml.edu/IRTAM/) described in [8].

With regard to this, in Fig. 3 a comparison among measured values, and those calculated by IRI (here with IRI we mean the IRI model with the storm option set to on), IRI UP , and IRTAM models, is shown for foF2. In the first and third panel from the top are shown the foF2 time series registered from the ionosonde (blue line), calculated by IRI (green line), IRI UP (red line), and IRTAM (cyan line), for Fairford and San Vito test stations, respectively. Second and fourth panels from the top show time series of the differences between values registered from the ionosonde and calculated respectively by IRI (blue line), IRI UP (green line) and IRTAM (red line), for Fairford and San Vito test stations. Statistical quantities related to these time series are shown in Tab. 1.

Time series in Fig. 3 show: a general underestimation of foF2 made by IRI for quiet conditions, before the storm commencement (March 17) and in the last part of the time series; a general overestimation under disturbed conditions in the recovery phase of the storm (March 19-22); an important underestimation in the main phase of the storm (March 17-18). This feature is clearly evident for Fairford (second panel from the top), whilst a more wavy behavior, under quiet days, holds for San Vito station (fourth panel from the top). The STORM option in the IRI model, for this particularly severe event, appears to be insufficient to represent such an ionospheric weather event. On the other hand, both IRI UP and IRTAM show a better agreement with the measured values. The IRTAM model, although it is very efficient for quiet days, it displays some deficiencies in the main phase of the storm. For example, at Fairford on March 18, IRTAM shows a general overestimation of the foF2 values, while this is not the case for IRI and IRI UP. For the same time window, at San Vito, IRTAM shows a general underestimation, even though less pronounced than that shown by IRI. This particular day (March 18), under very severe disturbed conditions, clearly demonstrate that during the main phase of the storm the ionosphere is really spatially variable, with very different values of foF2 for Fairford and San Vito. This spatial variability is well represented by the IRI UP model, whose behavior is good both for quiet and, more important, for disturbed conditions. The spatial description of the effective indices, through the universal Kriging spatial interpolation method, appears to be very effective for foF2, allowing to describe the different effects that the storm has on different latitudes. This is supported by the statistical quantities shown in Tab.1. Statistical distributions of the differences between each model and measured values (not shown here) further highlight how IRI UP model performs well, with distributions highly picked around the zero and very small dispersion values than those associated with IRI and IRTAM. IRTAM has a good accuracy but with a less degree of precision than the IRI UP model.

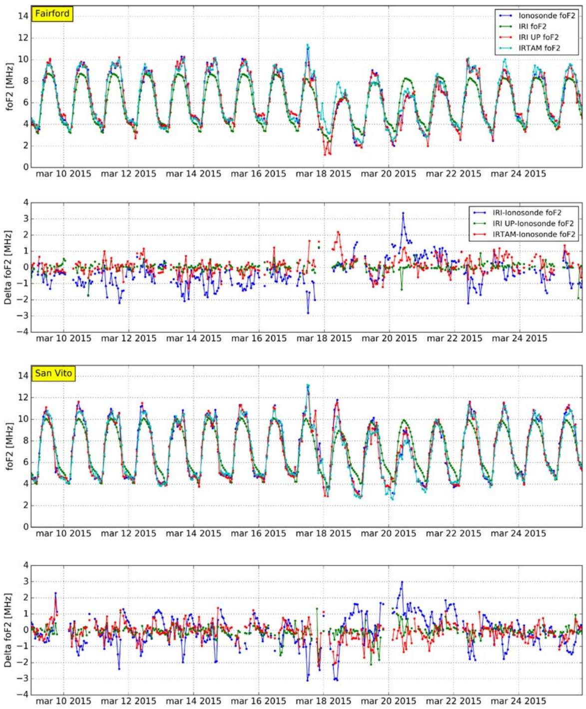

Fig.3: Comparison between measured values of foF2, and foF2 values calculated by IRI, IRI UP and IRTAM models.

		Comparison	RMSE	NRMSE	Corr. Coeff.	Mean delta	Sta. Dev. Delta
Fairford	foF2	Iono. vs IRI	0.92 MHz	13.81 %	0.93	-0.35 MHz	0.85 MHz
		Iono. vs IRI UP	0.26 MHz	3.90 %	0.99	0.02 MHz	0.27 MHz
		Iono. vs IRTAM	0.53 MHz	8.07 %	0.97	0.11 MHz	0.52 MHz
San Vito	foF2	Iono. vs IRI	0.95 MHz	12.82 %	0.94	-0.05 MHz	0.95 MHz
		Iono. vs IRI UP	0.37 MHz	5.02 %	0.99	-0.08 MHz	0.38 MHz
		Iono. vs IRTAM	0.56 MHz	7.55 %	0.98	-0.10 MHz	0.55 MHz
Fairford	hmF2	Iono. vs IRI	22.23 km	7.61 %	0.84	2.65 km	22.07 km
		Iono. vs IRI UP	11.57 km	3.96 %	0.94	-0.44 km	13.78 km
		Iono. vs IRTAM	13.72 km	4.70 %	0.94	-2.22 km	13.54 km
San Vito	hmF2	Iono. vs IRI	19.69 km	6.72 %	0.86	2.67 km	19.51 km
		Iono. vs IRI UP	13.57 km	4.63 %	0.92	-5.34 km	15.44 km
		Iono. vs IRTAM	14.48 km	4.94 %	0.93	1.07 km	14.44 km

Tab 1: Statistical results of the comparison between foF2 measured values (Iono) and those calculated by IRI, IRI UP, and IRTAM models.

An analogous analysis of the hmF2 time series (not shown here) shows a very distinct behavior between quiet-moderate and high disturbed conditions. In fact, compared to the smooth behavior under quiet and moderate-disturbed days, under very disturbed conditions (March 17) hmF2 values are very variable from an hour to another with very big differences. The statistical values of Tab.1 calculated for hmF2 show that both IRI UP and IRTAM improve IRI performance, but now with a small difference to the advantage of IRTAM model.

References

1. Bilitza D., Altadill D., Zhang Y., Mertens C., Truhlik V., Richards P., McKinnell L.A., Reinisch B., “The International Reference Ionosphere 2012 – a model of international collaboration”. *J. Space Weather Space Clim.*, Vol.4, A07, 2014.

2. Araujo-Pradere E.A., Fuller-Rowell T.J., Codrescu M.V., “STORM: An empirical storm-time ionospheric correction model 1. Model description”. *Radio Science*, Vol.37 N.5, 1070, 2002.

3. Pignalberi A., Pezzopane M., Tozzi R., De Michelis P., Coco I. (2016): Comparison between IRI and preliminary Swarm Langmuir probe measurements during the St. Patrick storm period. Earth, Planets and Space, 68:93.

4. Jones W.B., Gallet R.M., “Representation of diurnal and geographical variations of ionospheric data by numerical methods”. *Telecommunication Journal*, Vol.29, 129-149, 1962.

5. Bilitza D., Sheikh M., Eyfrig R., “A global model for the height of the F2-peak using M3000 values from the CCIR numerical map”. *Telecommunication Journal*, Vol.46, 549-553, 1962.

6. Matheron G., “Principles of geostatistics”. *Economic geology*, Vol.58, 1246-1266, 1963

7. Kitanidis P.K., “Introduction to geostatistics: application to hydrogeology”. *Cambridge University Press,* 1997.

8. Galkin I.A., Reinisch B.W., Huang X., Bilitza D., “Assimilation of GIRO data into a real-time IRI”. *Radio Science*, Vol.47 RS0L07, 2012.